Crop Detection and Individual Nozzle Simulation and Activation Using Monocular Vision

Henrique Gonçalves Andrade * **Gustavo Henrique do Nascimento** ** **Paulo Lilles Jorge Drews Jr** ***

* *Núcleo de Inovação em Máquinas e Equipamentos Agrícolas, Universidade Federal de Pelotas, RS, (e-mail: henrique.andrade@ufpel.edu.br).*
** *Centro de Ciências Computacionais, Universidade Federal do Rio Grande, RS, (e-mail: gus_nascimento98@hotmail.com)*
*** *Centro de Ciências Computacionais, Universidade Federal do Rio Grande, RS, (e-mail: paulodrews@furg.br)*

Abstract: The present works brings the development of a perception system for crop detection, activation of a single nozzle and simulation for a pesticide sprayer. The purpose is to embed the system on the agricultural machine to avoid the waste of pesticide by applying it only where it is necessary, being less aggressive with the soil. Our motivation is to implement simply advanced technique capable of being adopted by family farmers, with low cost and high efficiency. There is a hardware cost limitation, such as the use of a single camera to the proposal's motivation of being viable for family farmers. Its implementation occurs by using simple hardware that runs computer vision software that applies crop row detection techniques and triggers logic to the nozzles. The results showed that the proposal can identify the crops and activate each nozzle individually. However, the processing time test shows that the algorithm needs an implementation improvement.

Keywords: Perception and sensing; Computer vision; Agricultural robotics; Agricultural automation; Embedded system.

1. INTRODUCTION

According to the UN, the global population is growing and it consequently increases the demand for food. Therefore, a new concept of agriculture emerged, called precision farm, which focuses on a junction between productivity and sustainability.

Some pests like insects and invasive plants cause significant losses of production, and the farmers apply pesticides to their crops to avoid the problem. However, the solution creates other problems like health risks for the workers and contamination of the ecosystem. Ribeiro et al. (2007) elucidates that the lost in extreme cases is more than 90% of the pesticide applied and does not act on the field.

According to Machado et al. (2005), there are many ways to apply pesticides on the crop that consider important factors as biological knowledge of the target; the use of the right product and the machinery used in the application. The pesticide can be found in the solid, liquid or gaseous state, and the liquid one is the most used in agriculture through techniques such as nebulization, atomization, spraying, injection, immersion or brushing.

In this work, the focus is on the spray technique. In the market, there are a lot of machines that perform this activity such as coastal, self-propelled and bar sprayers. We base this work on the operation of a boom sprayer.

Some solution for solving the problem of the non-optimized use of pesticides are found in the literature such as in Terra et al. (2020). The authors use low-cost microprocessors to individualize the actuation of the nozzles of a boom sprayer. It shows that their system can detect lines in plantations and it can be used to retrofit conventional boom sprayers. do Nascimento et al. (2019) proposed a system to identify plants in the field using modern cameras and technologies, concluding it as a robust method. Ferreira (2017) achieved 98% accuracy using deep neural networks to identify invasive plants in soybean crops.

Winterhalter et al. (2018) detected planting lines of small plants using the pattern Hough transform. They collected visual data using a five-megapixel PointGrey Blackfly camera to detect small plants and a Nippon-Signal FX-8 3d laser to detect large ones. The authors show that their algorithm provides reliable and accurate results.

The focus in this article is to use low-cost technologies and ensure efficient results, proposing a system capable of detecting crop lines and simulating the individual activation of the nozzles via software. The algorithm identifies the lines through computer vision techniques on images captured by a conventional camera, acting on embedded hardware. In parallel to this functionality, the system also aims to identify possible improvements in the software. A

⋆ We would like to acknowledge CAPES and CNPq for the founding to research.

functional abstraction image of the system can be seen in Fig. 1.

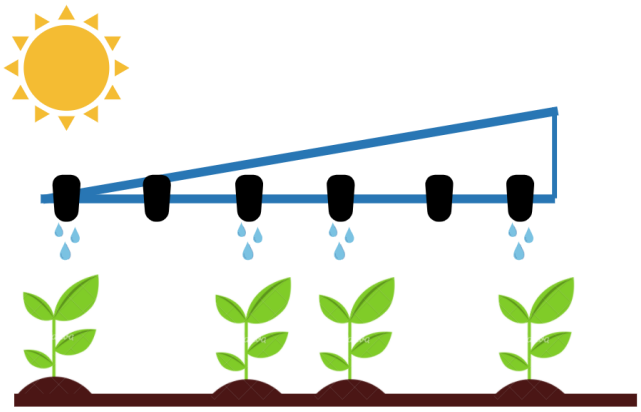

Figure 1. Abstraction of the individual actuation of the nozzles.

2. METHODOLOGY

The methodology is divided in two parts: the Crop Detection and Nozzle Simulation, and Single Nozzle Activation. There is a perception system and a control system. The perception system begins to detect when it is turn up. This is done by taking each frame of the video, and the crops are identified through computer vision techniques. After the identification, the same system simulates the state of the nozzles on the pesticide boom sprayer - the Crop Detection and Nozzle simulation. The Single Nozzle Activation acts with the state change corresponding nozzle from the simulation. The control system is responsible for this activation.

The embedded system has the goal of working with only a fraction of the boom sprayer bar, thus, there will be many systems, and each one will be responsible for a specific set of nozzles. The height of the camera's position will define the size of the set. The perception system must me able to communicate with the control system to trigger the correct nozzles.

In the first stage, the perception system algorithm follows the sequence present on the flowchart in Fig. 2, divided in four parts: Region of Interest, Segmentation, Preprocessing and Crop Detection.

Fundamentally, the algorithm aims to raise the efficiency by decreasing the processing time of the segmentation, so it closes the Region of Interest to take only 25% of the image's bottom instead of working with 100% because the essential data is in the region near the boom sprayer, where the application of the pesticide will proceed.

Subsequently, there are two segmentation methods tested, the Excess of green by Woebbecke et al. (1995) and the excess of green minus excess of red minus excess of blue by Underwood et al. (2015). We used the first simulation in a controlled environment and the second one in a video recorded in an onion crop.

Woebbecke et al. (1995) showed in their article a comparison of some contrast indices, and the conclusion was that the best one to separate plants from background was the

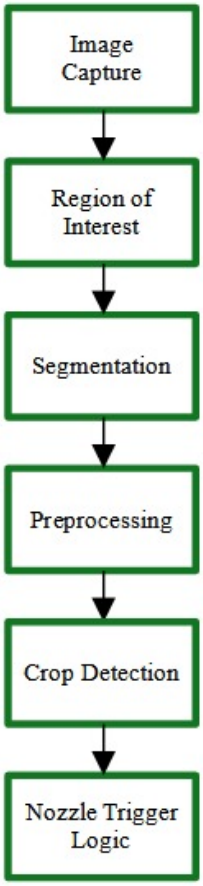

Figure 2. Perception System Flowchart.

Excess of Green. Its application occurs by amplification on the green channel and subtracting the red and the blue channel (1).

$$Ex_g = 2G - R - B \tag{1}$$

Where G, R, and B are the respective green, red and blue input image channels.

Underwood et al. (2015) proposed in their article a segmentation called Excess of Green minus Excess of Red minus Excess of Blue (Ex_{grb}). This segmentation occurs by verifying two conditions, present in (2) and (3). We can adjust the parameters k and t, and their values will define the hue of green.

$$G > k(R + B) \tag{2}$$

$$(R + B) > t \tag{3}$$

Where B, G, and R are the color channels of the image and the parameters k and t which values are respectively 0.62 and 40.

On the preprocessing state, we apply the morphological operations of erode and dilate.The erosion operation is to remove the noise of the image and the dilatation operation is to highlight the data.

Afterward, we implement the crop detection logic. The number of nozzles that the perception system will be able to be responsible for defines an image divided into n regions vertically, and a horizontal line. If there are pixels to be considered to be from the crop above the horizontal line, there is a change of the state of the nozzle that belongs to the respective region from closed to open.

Finally, the activation of the nozzles occurs on the Nozzle Trigger Logic. It happens by a communication between the perception system and embedded system responsible to trigger the relays that activate the nozzles. The perception system will be sending the index and the status of the nozzles after which frame to the control system.

2.1 Experiments

There are two stages of the conduction of the experiments: test and validation. The test occurs in a controlled environment where the crop is simulated to verify the conduct of the perception system. To validate the system, it uses a video recorded on an actual crop.

Firstly, building a prototype to test the algorithm and the system. A Logitech C922 camera and a Nvidia Jetson Nano compose the hardware, as in Fig. 3. There is the placement of the camera on a platform to do the experiments. The platform has a height of $45mm$ and its angle with the platform is 99^o, as in Fig. 4.

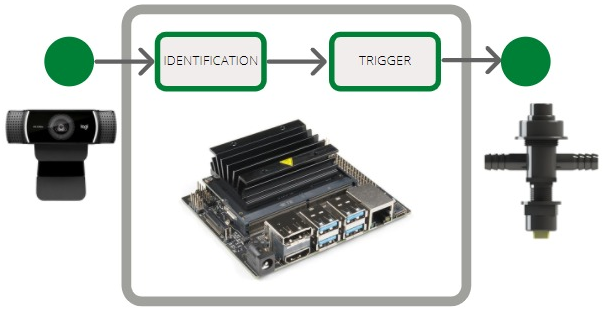

Figure 3. Hardware composition.

Figure 4. Platform.

We use the platform to test the system in a controlled environment. There is the replication of the planting lines on a table with Mate herb to simulate the crop row, in an area of $32cm^2$, as in Fig.5.

We use the platform to test the system in a controlled environment. There is the replication of the planting lines on a table with Mate herb to simulate the crop row, in an area of, as in Fig. 6 and run into Zhang's algorithm, Zhang (2000). We use 20 images of the chessboard with the dimensions of $20mm \times 20mm$ to do that.

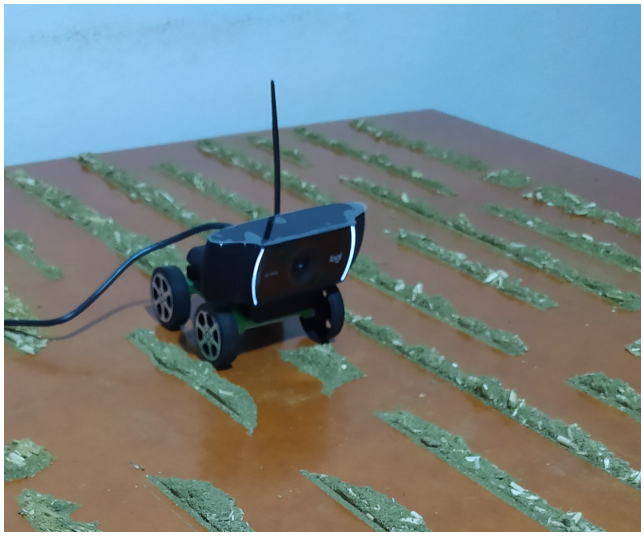

Figure 5. Experiment setup.

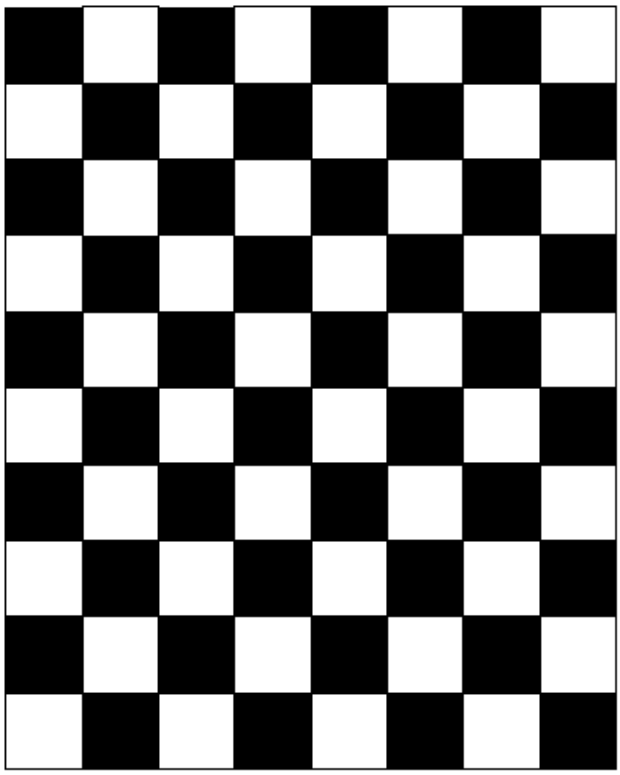

Figure 6. Chessboard.

The camera matrix (P) represents the transformation of a dot (Q) from a $3D$ space to a dot (q) on the $2D$ image's plane (4) is the result of the algorithm.

$$q = PQ \tag{4}$$

The camera's matrix, represented in (5), gives internal optical and geometric characteristics of the camera as focal

length, f_x and f_y, and the pixel position of the orthogonal projection of the optical center in the projection plane, c_x and c_y.

$$P = \begin{bmatrix} f_x & 0 & c_x \\ 0 & f_y & c_y \\ 0 & 0 & 1 \end{bmatrix} \quad (5)$$

The distortion coefficient vector in (6) gives the values that represent the quantity of the radial and tangential distortion in an image.

$$Distortion\ coefficients = [k_1\ k_2\ p_1\ p_2\ k_3] \quad (6)$$

We perform a second experiment with a time test that subjects each session of the code. Hence, we took a video frame and submitted it to processing on the Jetson Nano board. There are 3 repetitions of the procedure (Rep.1, Rep.2 and Rep.3) and at the end, we calculate the average of each session of the code, as well as the total average of the elapsed time. We do this for both conditions established in that work (controlled and on the field).

To evaluate the conduct of the algorithm in a real situation, we use a video recorded in the field with a generic camera. Therefore, there is no evaluation of the reconstruction stage in this experiment, but there is the evaluation of the same perception system's algorithm.

3. RESULTS

Foremost, the calibration procedure is the first step to starts the simulation on the controlled environment, and the result is the matrix (7) that shows the intrinsic parameter of the camera.

$$P = \begin{bmatrix} 1260 & 0 & 625 \\ 0 & 1257 & 335 \\ 0 & 0 & 1 \end{bmatrix} \quad (7)$$

Besides the camera matrix, we obtain the camera's distortion coefficients, which represent the extrinsic parameters of the camera.

- $k_1 = 0.03902417$
- $k_2 = -0.00412822$
- $p_1 = -0.00374443$
- $p_2 = 0.00342203$
- $k_3 = -0.22578201$

In the experiment, there is the application of the procedure to the two present segmentations to evaluate the processing time and the robustness of the techniques on the studied case.

The controlled environment's test of the system presented the following results. The first step of the algorithm takes the Region of Interest that is shown in Fig. 7.

To the segmentation step, we use the technique by Woebbecke et al. (1995), which results are present in Fig. 8.

There is the application of the morphological operations to the preprocessing. The morphological shape of the erode

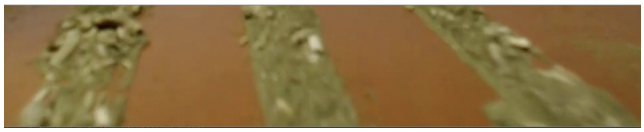

Figure 7. Region of Interest on the controlled environment.

Figure 8. Segmentation on the controlled environment.

and the dilate kernel are rectangular and their respective size is: 3×3 and 5×5. The result is presented in Fig. 9.

Figure 9. Morphological Operations on the controlled environment.

The next step is the creation of the horizontal line in the X-axis of the dilated images, which detects if there is a crop in that region and then generates the trigger signals. We draw this line on the X-axis at 10% of the dilated image's height, as in Fig. 10. It is possible to notice on the same figure the simulation elements where the green circle represents the activated nozzle and the red circle indicates the deactivated nozzle.

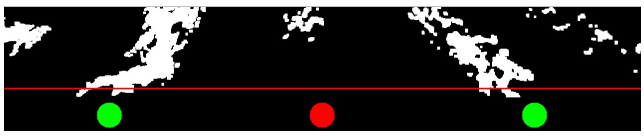

Figure 10. Trigger signals in a controlled environment.

Next, there is the performing of the processing time for the experiment under controlled conditions. The results are in Table 1 and the measurement unit is milliseconds.

Table 1. Processing time of each session of the code in a controlled environment.

Session	Rep.1	Rep.2	Rep.3	Average
Reconstruction	246.63	248.37	247.24	247.41
Cut	0	0	0	0
Segmentation	5.03	5.06	5.05	5.04
Binarization	1.96	1.73	1.3	1.66
Erosion	7.3	7.32	7.54	7.38
Dilatation	12.16	12	12.16	12.10
Trigger	871.56	922.23	894.5	896.1
Total	1144.64	1196.71	1167.79	1169.69

The average frame processing time is 1169.63 milliseconds, where the Trigger is the slowest function representing 76.61% of the total average time followed by the reconstruction (21.15%).

The results of the test performed with the frame of a video in real field conditions are in Fig. 11. It is possible to see the cropped image in the region of interest.

Figure 11. Image cropped.

The result of the segmentation using the proposal of Underwood et al. (2015) represented in Fig. 12.

Figure 12. Segmentation by green excess of the cropped image.

The result of the morphological operations of erosion and dilatation are in Fig. 13.

The Fig. 14 presents the nozzle activation on the crop image.

The table 2 presents the values of time processing in milliseconds for each session of the code running in a NVIDIA Jetson Nano development kit.

It is possible to observe that for each frame the algorithm takes about 1850.88 milliseconds to process, where the segmentation is the slowest session corresponding to 91.2% of the total time of process followed by the Trigger logic (8.6%).

Figure 13. Result of the morphological operations.

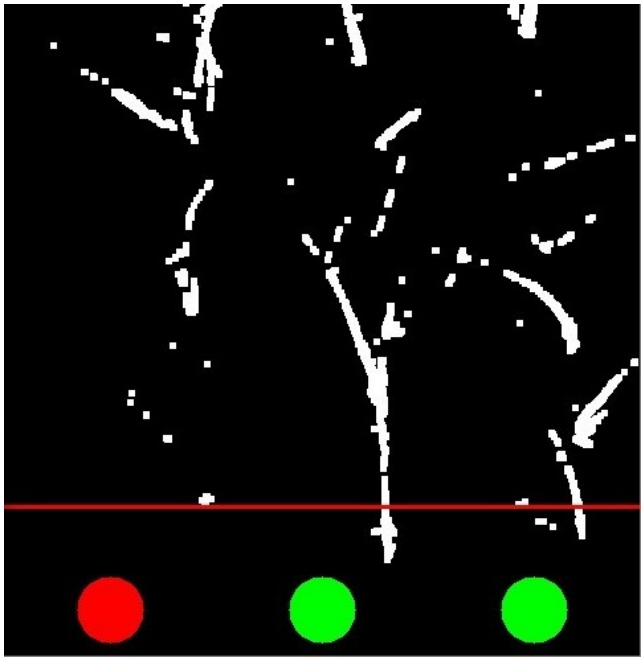

Figure 14. The trigger simulation.

4. CONCLUSION

The system proved to be functional, and capable of identifying crop lines and their failures with good performance in the individual activation of the nozzles. We improve the process altogether with the use of optimized features of the

Table 2. Processing time of each session of the code.

Session	Rep.1	Rep.2	Rep.3	Average
Cut	0	0	0	0
Segmentation	1782.43	1621.28	1660.43	1688.04
Binarization	0	0	0	0
Erosion	1.63	1.60	1.39	1.54
Dilatation	2.06	2.17	2.06	2.09
Trigger	157.51	161.16	158.96	159.21
Total	1943.63	1786.21	1822.84	1850.88

NVIDIA Jetson Nano development Kit, such as the use of the graphics processing unit (GPU).

In the analysis of the processing times, the segmentation strategy implemented based on the work of Woebbecke et al. (1995) proved to be faster than the strategy implemented based on the work of Underwood et al. (2015), and it might be because of the way we implemented it in our algorithm. Even though the first segmentation was faster than the other, the second segmentation presents more robustness in the open field environment.

The logic of triggering the nozzles proved to be very computationally expensive in both experiments due to the implementation, however, the logic proved to be efficient.

For future work, we aim to improve the system by using the resources available on the hardware, as well as enabling the communication of the system with the other devices through a CAN bus (Control Area Network). By adopting a new logic to activate the nozzles will optimize the software performance, and also improve the implementation of segmentation techniques.

ACKNOWLEDGEMENTS

We would like to acknowledge the AutoCeres project, where this work was born, for providing integration between institutions, and CAPES and CNPq institutions for providing financial support to keep researching. Finally, we would like to thank the family farmers who inspire this project to improve their quality of life.

REFERENCES

do Nascimento, G.H., Weber, F., Almeida, G., Terra, F.P., and Jr, P.L.J.D. (2019). A perception system for an autonomous pesticide boom sprayer. Latin American Robotics Symposium (LARS), 2019 Brazilian Symposium on Robotics (SBR) and 2019 Workshop on Robotics in Education (WRE).

Ferreira, A.S. (2017). *Redes neurais convolucionais profundas na detecção de plantas daninhas em lavoura de soja.* Mestrado, PPCC-UFMGS, Campo Grande, MS.

Machado, A.L.T., dos Reis, A.V., de Moraes, M., and Alonço, S.S. (eds.) (2005). *Máquinas para preparo do solo, semeadura, adubação e tratamentos culturais.* UFPel Universitária.

Ribeiro, M.L., Lourencetti, C., Pereira, S.Y., and dMarchi, M.R.R. (2007). Contaminação de águas subterrâneas por pesticidas: avaliação preliminar,. *Química Nova*, 30, 688–694.

Terra, F., do Nascimento, G., Duarte, G., and Drews-Jr, P. (2020). Autonomous agricultural sprayer using machine vision and nozzle control. *Journal of Intelligent and Robotic Systems.*

Underwood, J.P., Calleija, M., Taylor, Z., Hung, C., Nieto, J., Fitch, R., and Sukkarieh, S. (2015). Real-time target detection and steerable spray for vegetable crops. *International Conference on Robotics and Automation (ICRA), Workshop on Robotics in Agriculture.*

Winterhalter, W., Fleckenstein, F.V., Dornhege, C., and Burgard, W. (2018). Crop row detection on tiny plants with the pattern hough transform. *IEEE Robotics and Automation Letters*, 3(4), 3394–3401.

Woebbecke, D.M., Meyer, G.E., Von Bargen, K., and Mortensen, D.A. (1995). Color indices for weed identification under various soil, residue, and lighting conditions. *Transactions of the ASAE*, 38(1), 259–269.

Zhang, Z. (2000). A flexible new technique for camera calibration. *IEEE Transactions on Pattern Analysis and Machine Intelligence*, 22(11), 1330–1334. doi:10.1109/34.888718.